

# Photocurable Pickering Emulsion for Colloidal Particles with Structural Complexity

Shin-Hyun Kim,<sup>†</sup> Gi-Ra Yi,<sup>‡</sup> Kyu Han Kim,<sup>†</sup> and Seung-Man Yang<sup>\*,†</sup>

National Creative Research Initiative Center for Integrated Optofluidic Systems and Department of Chemical and Biomolecular Engineering, Korea Advanced Institute of Science and Technology, Daejeon 305-701, and Korea Basic Science Institute, Seoul 136-713, Korea

Received October 1, 2007. In Final Form: November 29, 2007

We prepared polymeric microparticles with coordinated patches using oil-in-water emulsion droplets which were stabilized by adsorbed colloidal polystyrene (PS) latex particles. The oil phase was photocurable ethoxylated trimethylolpropane triacrylate (ETPTA), and the particle-armored oil droplets were solidified by UV irradiation within a few seconds to produce ETPTA–PS composite microparticles without disturbing the structures. Large armored emulsion drops became raspberry-like particles, while small emulsion drops with a few anchored particles were transformed into colloidal clusters with well-coordinated patches. For high-molecular-weight PS particles with low chemical affinity to the ETPTA monomer, the morphology of the patchy particle was determined by the volume of the emulsion drop and the contact angle of the emulsion interface on the PS particle surface. Meanwhile, for low-molecular-weight PS particles with high affinity, the ETPTA monomers were likely to swell the adsorbed PS particles, and distinctive morphologies were induced during the shrinkage of emulsion drops and the phase separation of ETPTA from the swollen PS particles. In addition, colloidal particles with large open windows were produced by dissolving the PS particles from the patchy particles. We observed photoluminescent emission from the patchy particles in which dye molecules were dispersed in the ETPTA phase. Finally, we used Surface Evolver simulation to predict equilibrium structures of patchy particles and estimate surface energies which are essential to understand the underlying physics.

## Introduction

Colloidal particles have been studied as atomic and molecular model systems due to their phase behavior. Isotropic, monodisperse colloids yield various crystalline structures depending on the interparticle potential, such as a face-centered cubic (fcc), a body-centered cubic (bcc), and a hexagonal close-packed (hcp) structure.<sup>1,2</sup> Recently, Bartlett et al. and Leunissen et al. showed experimentally and theoretically that bidisperse colloidal systems with opposite charges enable unconventional crystalline structures such as CsCl, NaCl, and assemblies of bimodal colloids to be made.<sup>3,4</sup> In addition, self-organization of anisotropic colloids has been a demanding issue in the areas of functional colloidal structures including colloidal crystals of a diamond lattice with robust photonic band gaps.<sup>5–8</sup>

One of the typical strategies for preparing anisotropic particles is based on the lithographic technique. A photoresist, which is film cast on a wafer or flows in a microfluidic channel, is selectively exposed by UV or visible light through a photomask, and subsequent development leaves behind anisotropic particles.<sup>9–13</sup> However, this method has some drawbacks such as low

throughput and limitation in material properties. Another strategy is based on colloidal emulsions and particles. For example, ellipsoidal polymeric particles can be obtained by stretching the spherical polymeric particles which are embedded in a flexible matrix above the glass transition temperature.<sup>14–16</sup> Also polymer microrods with high aspect ratios can be produced by the liquid–liquid dispersion technique developed by Alargova et al.,<sup>17</sup> and dumbbell-shaped particles can be synthesized by protruding the monomers from the swollen seed particles in a modified seeded emulsion or dispersion polymerization.<sup>18–21</sup> In addition, spherical particles with anisotropic surface properties have been prepared by using microcontact printing,<sup>22</sup> the gel trapping technique at the liquid interface,<sup>23</sup> and a colloidal shadow mask in multilayered colloidal crystals.<sup>24</sup>

Recently, colloidal clusters with unique configurations of dense packing were prepared by evaporating the oil phase from oil-in-water emulsion drops in which colloidal microspheres were bound to the interface.<sup>25,26</sup> More recently, colloidal clusters with coordinated patches were synthesized by adding some consoli-

\* To whom correspondence should be addressed. E-mail: smyang@kaist.ac.kr.

<sup>†</sup> Korea Advanced Institute of Science and Technology.

<sup>‡</sup> Korea Basic Science Institute.

- (1) Kegel, W. K.; van Blaaderen, A. *Science* **2000**, *287*, 290–293.
- (2) Yethiraj, A.; van Blaaderen, A. *Nature* **2003**, *421*, 513–517.
- (3) Bartlett, P.; Campbell, A. I. *Phys. Rev. Lett.* **2005**, *95*, 128302.
- (4) Leunissen, M. E.; Christova, C. G.; Hynninen, A. P.; Royall, C. P.; Campbell, A. I.; Imhof, A.; Dijkstra, M.; van Roij, R.; van Blaaderen, A. *Nature* **2005**, *437*, 235–240.
- (5) Glotzer, S. C. *Science* **2004**, *306*, 419–420.
- (6) Zhang, Z. L.; Glotzer, S. C. *Nano Lett.* **2004**, *4*, 1407–1413.
- (7) Zhang, Z. L.; Keys, A. S.; Chen, T.; Glotzer, S. C. *Langmuir* **2005**, *21*, 11547–11551.
- (8) Bianchi, E.; Largo, J.; Tartaglia, P.; Zaccarelli, E.; Sciortino, F. *Phys. Rev. Lett.* **2006**, *97*, 168301.
- (9) Badaire, S.; Cottin-Bizonne, C.; Woody, J. W.; Yang, A.; Stroock, A. D. *J. Am. Chem. Soc.* **2007**, *129*, 40–41.
- (10) Dendukuri, D.; Pregel, D. C.; Collins, J.; Hatton, T. A.; Doyle, P. S. *Nat. Mater.* **2006**, *5*, 365–369.

- (11) Hernandez, C. J.; Mason, T. G. *J. Phys. Chem. C* **2007**, *111*, 4477–4480.
- (12) Pregel, D. C.; Toner, M.; Doyle, P. S. *Science* **2007**, *315*, 1393–1396.
- (13) Xu, S. Q.; Nie, Z. H.; Seo, M.; Lewis, P.; Kumacheva, E.; Stone, H. A.; Garstecki, P.; Weibel, D. B.; Gitlin, I.; Whitesides, G. M. *Angew. Chem., Int. Ed.* **2005**, *44*, 724–728.
- (14) Ho, C. C.; Hill, M. J.; Odell, J. A. *Polymer* **1993**, *34*, 2019–2023.
- (15) Lu, Y.; Yin, Y. D.; Xia, Y. N. *Adv. Mater.* **2001**, *13*, 271–274.
- (16) Nagy, M.; Keller, A. *Polym. Commun.* **1989**, *30*, 130–132.
- (17) Alargova, R. G.; Bhatt, K. H.; Paunov, V. N.; Veleev, O. D. *Adv. Mater.* **2004**, *16*, 1653–1657.
- (18) Sheu, H. R.; Elaissar, M. S.; Vanderhoff, J. W. *J. Polym. Sci., Part A: Polym. Chem.* **1990**, *28*, 629–651.
- (19) Mock, E. B.; De Bruyn, H.; Hawke, B. S.; Gilbert, R. G.; Zukoski, C. F. *Langmuir* **2006**, *22*, 4037–4043.
- (20) Kegel, W. K.; Breed, D.; Elsesser, M.; Pine, D. J. *Langmuir* **2006**, *22*, 7135–7136.
- (21) Kim, J. W.; Larsen, R. J.; Weitz, D. A. *J. Am. Chem. Soc.* **2006**, *128*, 14374–14377.
- (22) Cayre, O.; Paunov, V. N.; Veleev, O. D. *Chem. Commun.* **2003**, 2296–2297.
- (23) Paunov, V. N.; Cayre, O. *Adv. Mater.* **2004**, *16*, 788–791.
- (24) Zhang, G.; Wang, D. Y.; Mohwald, H. *Angew. Chem., Int. Ed.* **2005**, *44*, 7767–7770.

dative substances such as nanoparticles or polymers in the emulsion drop phase.<sup>27,28</sup> The nanoparticles or polymers covered clusters of colloidal microspheres with some exposed parts (i.e., patches) during evaporation of the drop phase and consolidated the colloidal structures. The patchy particles can be used as building blocks for novel colloidal structures because the exposed patches may induce directional interactions. However, the evaporation-induced self-assembly required long times and high temperature, and alternative methods of rapid and reliable consolidation are still needed for colloidal patchy particles.

In this study, we demonstrate the preparation of anisotropic microparticles with well-coordinated patches using particle-stabilized oil-in-water emulsions in which the oil phase is photocurable. In particle-stabilized Pickering emulsions or bubbles, the colloidal particles are adsorbed on the liquid–liquid or liquid–gas interface to reduce the surface energy. In particular, when the particles are bound to the interface strongly, only tangential movement is allowed with a constant contact angle which determines the position of the contact line.<sup>29–32</sup> If the emulsion drop is photocurable and stabilized with adsorbed particles without any consolidating additives, the structure can be captured by UV irradiation in a few seconds.<sup>33</sup> In our previous paper, we showed that a photocurable Pickering emulsion is useful for investigating the interface morphologies and properties.<sup>34</sup> Specifically, we examined here the structures of colloidal clusters, which were partially covered with photocured acrylate resin of ethoxylated trimethylolpropane triacrylate (ETPTA), and their various derivatives of different morphologies. In doing this, we first emulsified the ETPTA resin into an aqueous medium which contained monodisperse colloidal polystyrene (PS) particles. Then, the PS particles were adsorbed spontaneously on the emulsion interface to reduce the total interfacial energy, forming so-called Pickering emulsions. Finally, the structures of the particle-stabilized Pickering emulsion droplets were captured by UV curing of the ETPTA resin. We also performed numerical simulations using Surface Evolver to determine not only the particle configuration of a colloidal cluster but also the shape of the consolidating polymer surface by minimizing the total surface energy. Unlike conventional evaporation-induced clustering, photopolymerization of the emulsion drops produced colloidal clusters with structural complexity in a few seconds. In particular, when the ETPTA monomers were absorbed into and swelled the colloidal PS particles, odd-shaped composite clusters were produced. In addition, the colloidal PS particles were dissolved selectively from the ETPTA–PS composite clusters, leaving behind microparticles with coordinated large open windows. In the subsequent sections, we describe experimental details for fabricating the colloidal clusters of PS microspheres with various structures and discuss the morphologies of both the Pickering emulsion droplets and the photocured microparticles in terms of the interfacial energy and the volume of the ETPTA drop.

## Experimental Section

**Materials.** Three different PS particles were used in this experiment. PS particles of 2.1  $\mu\text{m}$  in average diameter, which were stabilized by sulfate groups, were purchased from Interfacial Dynamics (7–2200). PS particles of 2.2 and 2.1  $\mu\text{m}$  in average diameters were synthesized without cross-linker by dispersion polymerization and stabilized by amine and carboxyl groups, respectively.<sup>35,36</sup> In dispersion polymerization, azobisisobutyronitrile (AIBN; Junsei), octylphenol ethoxylate (Triton X-305, Fluka), poly(vinylpyrrolidone) (PVP;  $M_w \approx 55\,000$  and  $360\,000$ , Aldrich), acrylic acid (Sigma-Aldrich), 2-aminoethyl methacrylate hydrochloride (AEMH; Sigma-Aldrich), styrene monomer (Sigma-Aldrich), and ethanol (Merck) were used. ETPTA (SR454, Sartomer) and 2-hydroxy-2-methyl-1-phenyl-1-propanone (HMPP; Darocur 1173, Ciba Chemical) were used as a UV-curable oil and a photoinitiator, respectively. Toluene (Aldrich) was used to dissolve the PS particles selectively, and rhodamine B isothiocyanate (Aldrich) was used as a dye molecule. Tetrahydrofuran (THF; DC Chemical) was used to measure the molecular weight of PS in gel permeation chromatography.

**Synthesis of PS Particles.** During dispersion polymerization, amine and carboxyl groups were introduced into the 2.2 and 2.1  $\mu\text{m}$  PS particles by adding comonomers AEMH and acrylic acid, respectively, to adjust the chemical affinity to the ETPTA resin. For amidine PS particles, styrene monomer (6.87 mL), AIBN (0.25 g) as an initiator, PVP ( $M_w \approx 55\,000$ , 1 g) as a stabilizer, TX-305 (0.35 g) as a costabilizer, and AEMH (0.0094 g) as a comonomer were dispersed in ethanol (23.8 mL), and the mixture was deoxygenated by bubbling of nitrogen gas at room temperature for 30 min. Reaction took place in a 100 mL flask immersed in an oil bath at 70 °C with stirring at 100 rpm for 24 h. For PS with a carboxyl group, styrene monomer (3.3 mL), AIBN (0.12 g), PVP ( $M_w \approx 360\,000$ , 0.135 g), TX-305 (0.15 g), and acrylic acid (0.16 g) were dispersed in a mixture of ethanol (30.13 mL) and water (1.25 mL), and dispersion polymerization proceeded at the same reaction condition as used for synthesizing amidine PS particles. The resulting particles were washed several times and redispersed in water.

**Preparation of Emulsion Droplets and Solidification by UV Exposure.** UV-curable ETPTA was used as the dispersed oil phase with HMPP as a photoinitiator. The aqueous suspension of PS particles did not contain any stabilizer. Oil-in-water emulsion droplets were formed from a mixture of the ETPTA (500  $\mu\text{L}$ ) and aqueous suspension (12 mL, 5 vol %) of PS particles in a homogenizer (Heidolph, Silentcrusher M) with a rotor speed at 16 000 rpm for 1 min. Oil droplets were generated with diameters in the range of 1–100  $\mu\text{m}$ . The small colloidal PS particles adsorbed spontaneously on the drop surface to form a particle-stabilized Pickering emulsion. For colloidal clusters of a few PS particles, the size of the Pickering emulsion drops was reduced further by sonication for 2 min. To capture the morphology of the resulting Pickering emulsion droplets instantly, the emulsion was exposed directly to a broad UV light (mercury arc lamp) for 10 s. Solidified ETPTA droplets were rinsed with water, and large aggregates were separated and discarded. For ETPTA microparticles with large open windows, the aqueous suspension of ETPTA–PS composite particles with patches was centrifuged at 2000 rpm, and the composite particles were redispersed in toluene, which dissolved the PS particles selectively. To remove dissolved PS molecules, the samples were washed twice using toluene. For the dye-doped ETPTA phase, ETPTA (3 mL) and an ethanolic solution of rhodamine B (3 mL,  $10^{-4}$  M) were mixed, and finally ethanol was removed by evaporation at 70 °C in a convection oven.

**Characterization.** Images of the particle-stabilized emulsions were taken with an optical microscope (Nikon, TE2000-U), and UV-cured microparticles were observed via scanning electron microscopy (SEM) (Philips XL30). For SEM observation, the samples were coated with Au to render them conductive, and the acceleration voltage was 3–5 kV. The dye-doped clusters were observed through

(25) Manoharan, V. N.; Elssesser, M. T.; Pine, D. J. *Science* **2003**, *301*, 483–487.

(26) Lauga, E.; Brenner, M. P. *Phys. Rev. Lett.* **2004**, *93*, 238301.

(27) Cho, Y.-S.; Yi, G.-R.; Lim, J.-M.; Kim, S.-H.; Manoharan, V. N.; Pine, D. J.; Yang, S.-M. *J. Am. Chem. Soc.* **2005**, *127*, 15968–15975.

(28) Cho, Y.-S.; Yi, G.-R.; Kim, S.-H.; Jeon, S.-J.; Elssesser, M. T.; Yu, H. K.; Yang, S.-M.; Pine, D. J. *Chem. Mater.* **2007**, *19*, 3183–3193.

(29) Binks, B. P.; Lumsdon, S. O. *Langmuir* **2000**, *16*, 8622–8631.

(30) Pickering, S. U. *J. Chem. Soc.* **1907**, *91*, 2001–2021.

(31) Clint, J. H.; Taylor, S. E. *Colloids Surf.* **1992**, *65*, 61–67.

(32) Binks, B. P.; Lumsdon, S. O. *Phys. Chem. Chem. Phys.* **1999**, *1*, 3007–3016.

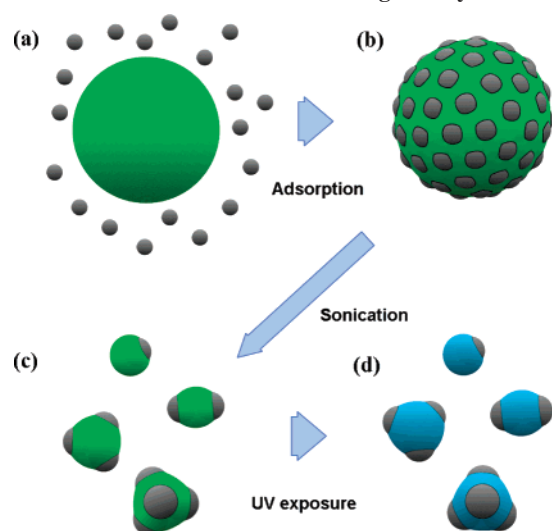
(33) Benkoski, J. J.; Hu, H.; Karim, A. *Macromol. Rapid Commun.* **2006**, *27*, 1212–1216.

(34) Kim, S.-H.; Heo, C.-J.; Lee, S. Y.; Yi, G.-R.; Yang, S.-M. *Chem. Mater.* **2007**, *19*, 4751–4760.

(35) Paine, A. J.; Luymes, W.; McNulty, J. *Macromolecules* **1990**, *23*, 3104–3109.

(36) Song, J. S.; Winnik, M. A. *Macromolecules* **2005**, *38*, 8300–8307.



Scheme 1. Schematic for Fabricating Patchy Particles<sup>a</sup>

<sup>a</sup> Small stabilizing particles were adsorbed on the surface of UV-curable oil drops, and the oil drops were broken into smaller ones by sonication. The small oil droplets with partially exposed particles were solidified by UV irradiation.

a laser scanning confocal microscope (Carl Zeiss, LSM 510). To measure the molecular weight of PS particles, we used gel permeation chromatography (GPC; 302-040 triple detector array, PC max module, OmniSEC 3.0 from Viscotek) with PS standards for GPC calibration.

## Results and Discussion

Recently, it has been demonstrated experimentally and theoretically that a few identical spherical particles captured on the interface of an oil-in-water emulsion drop are packed closely into a colloidal cluster during evaporation of the oil phase.<sup>25,26</sup> As the oil phase evaporates, the particles are jammed and form the critical packing that is a marginal configuration with a spherical emulsion interface. After the critical packing, capillary forces are exerted on the particles by the deformed interface, and the particles change their position to the final dense packing configuration. In this step, the shape of the emulsion interface is highly deformed from the spherical shape, and the oil phase evaporates completely in the end. One of the important features in the evaporation-induced assembly is that the cluster has a unique configuration depending only on the number ( $N$ ) of the constituting particles. A few examples of particle coordinations are touching two-particle aggregates for  $N = 2$ , triangles for  $N = 3$ , tetrahedrons for  $N = 4$ , triangular dipyramids for  $N = 5$ , octahedrons for  $N = 6$ , and pentagonal dipyramids for  $N = 7$ . These structures of clusters minimize the second moment of the mass distribution. Usually, the evaporation-induced self-organization of colloidal particles confined in emulsion drops proceeds quite slowly and takes over a few hours.

Meanwhile, in the case of a photocurable emulsion, the structures of the clusters can be captured within a few seconds by UV exposure. A schematic of our UV-induced fabrication of composite patchy particles is illustrated in Scheme 1. First, we prepared large Pickering emulsion drops of ETPTA stabilized by colloidal PS particles in an aqueous medium by homogenizing the ETPTA monomer resin in the aqueous PS suspension. For finer Pickering emulsion drops, the homogenized emulsions were sonicated and the subsequent UV exposure solidified the structures. The resulting clusters covered with the UV-cured ETPTA polymer had a few exposed patches; the number of patches was the same as the number  $N$  of the constituting particles. Parts a and b of Figure 1 are the typical optical microscope

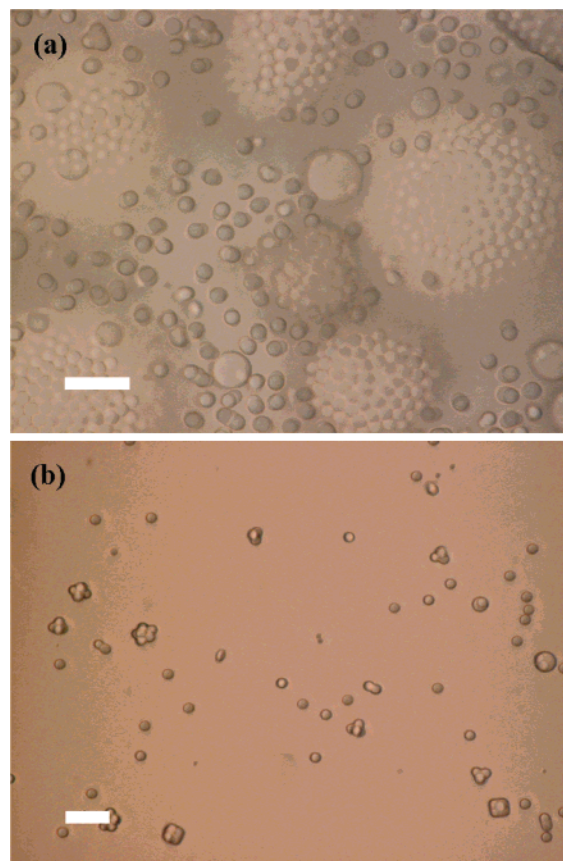


**Figure 1.** Optical microscope images of (a) large ETPTA drops covered with PS particles of  $2.2\ \mu\text{m}$  in diameter and (b) PS clusters partially covered with a small-volume ETPTA monomer drop. The scale bar is  $10\ \mu\text{m}$  in both images.

images of large Pickering emulsions before sonication and ETPTA-covered clusters after sonication, respectively. It can be seen from Figure 1a that the adsorbed PS particles on large ETPTA drops formed close-packed 2D shells while small drops contained a few PS particles. Usually, PS particles are stable in the aqueous phase due to the presence of tethered functional groups. However, a large portion of the surface still contains hydrophobic moieties due to the intrinsic characteristics of PS, and they are likely to anchor on the oil–water interface.<sup>37</sup> Large emulsion drops stabilized with the PS particles did not coalesce or break up unless strong external forces were exerted. During strong sonication, however, large ETPTA drops were broken into smaller ones and the adsorbed PS particles could be detached from the interface into the continuous water phase. The particle detachment was caused by the strong sonication energy which could overcome the particle binding energy and the lubrication resistance on the interface. From Figure 1b, we can see that colloidal clusters were formed in ETPTA drops of small volumes. In the following sections, we will discuss three types of the composite clusters from the photocurable Pickering emulsions and the energy reductions by the particle adsorption (or equivalently binding energies) estimated from Surface Evolver simulation.

**Composite PS Clusters Covered with ETPTA.** When the PS clusters partially covered by the ETPTA prepolymer resin are exposed to UV light, the ETPTA phase is solidified and patchy particles are generated. Therefore, the consolidated structures become stable under external stresses. Although the

(37) Velev, O. D.; Furusawa, K.; Nagayama, K. *Langmuir* **1996**, *12*, 2374–2384.

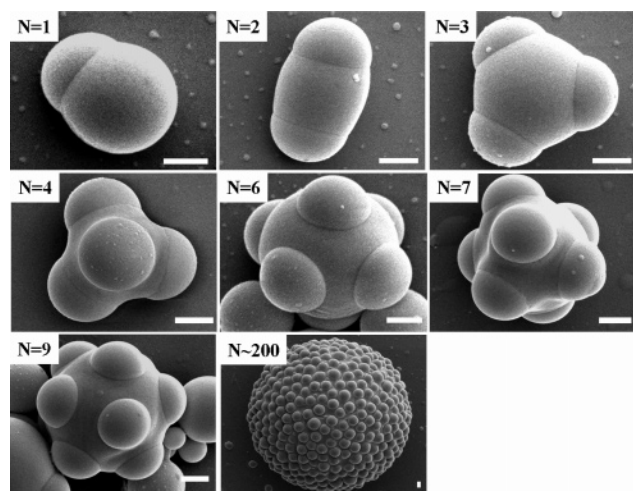


**Figure 2.** Collection of SEM images for patchy clusters and spherical assembly of PS particles with sulfate groups. The scale bar is 1  $\mu\text{m}$  in all images.

volume of the ETPTA monomer decreases slightly by 4% during photopolymerization, the degree of deformation is trivial. When we used PS particles with sulfate groups, we could obtain several types of colloidal clusters depending on  $N$ , the number of captured particles. Typical SEM images of patchy clusters of PS microspheres covered with ETPTA are shown in Figure 2. We can see clearly the contact lines on the PS particles from the SEM images. Since the surface property of the PS particles was uniform, the contact angle was constant and close to  $145^\circ$ . Because the ETPTA phase was nonvolatile with low diffusivity, the PS microspheres formed either close- or non-close-packed composite clusters depending on the initial volume of ETPTA resin. This volume-dependent particle configuration was different from the case in which the drop phase is evaporated to induce self-assembly. The pure patchy particles for  $N = 2$  or 4 with linear or tetrahedral coordination can be fractionated by density gradient centrifugation and used as building blocks with directional interactions.<sup>7</sup> Higher order patchy particles ( $N \geq 5$ ) are useful for the colloidal barcode system in combinatorial chemistry areas due to a large number of uncovered patches, which can be modified to interact selectively with target molecules.<sup>38–40</sup>

Because the ETPTA droplets were polydisperse in size, the patch size and obesity level of the composite clusters were not uniform for a given number of constituent PS particles. In Figure 3, SEM images of three different patchy clusters are shown for  $N = 2$  together with the corresponding model clusters of different emulsion volumes predicted by Surface Evolver simulation. Also included for comparison are the optical microscope images. In the Surface Evolver model clusters, two mesh spheres were point-contacted and the green-colored liquid phase showed the morphology of the minimal surface energy, which satisfied the constraints including the contact angle and the volume of the ETPTA drop.<sup>41</sup> Specifically, the contact angle was fixed at  $145^\circ$ , and the volume ratios of the liquid drop to the microsphere were 0.19, 0.43, and 0.61 for (a), (b), and (c), respectively. In Figure 3a, most of the particle surface is uncovered, while only half of the particle surface is exposed in Figure 3c. The optical microscope

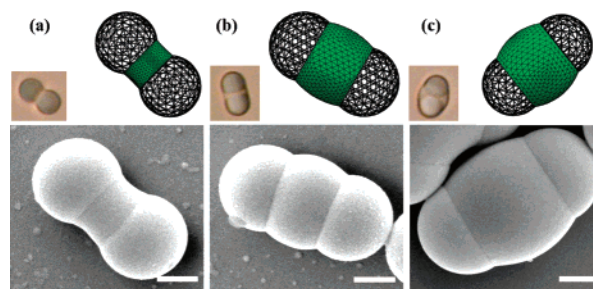


**Figure 3.** SEM and optical microscope images of patched clusters for  $N = 2$  and the corresponding Surface Evolver model images for (a)  $V/V_p = 0.19$ , (b)  $V/V_p = 0.43$ , and (c)  $V/V_p = 0.61$  at a  $145^\circ$  contact angle. The scale bar is 1  $\mu\text{m}$  in all images.

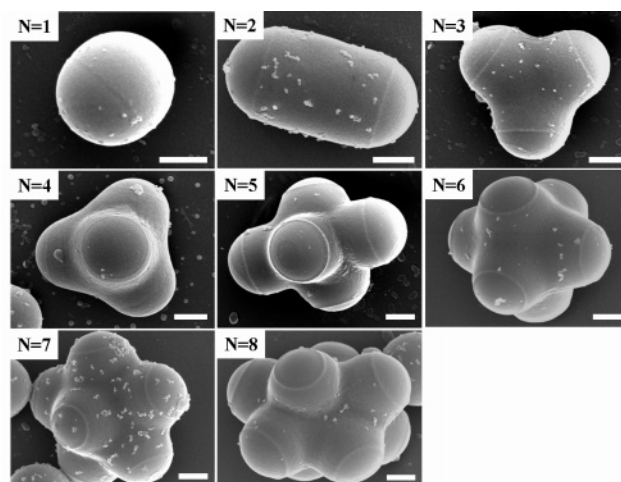


**Figure 4.** Collection of SEM images for patched clusters of amidine PS particles. The scale bar is 1  $\mu\text{m}$  in all images.

images show that the particles are contacting each other at one point and the ETPTA resin is covering the valley between two particles.

The ETPTA monomers can swell the PS particles, and different morphologies of the clusters can be induced depending on the degree of swelling. When we used amidine PS particles, the structures of the clusters were quite different from those for PS microspheres with sulfate groups shown in Figure 2. In Figure 4, the structural variety is summarized in terms of the number ( $N$ ) of constituting amidine PS microspheres. Up to  $N = 8$ , the particle configurations are quite similar to those of the minimal second moment clusters, which are unique dense packings for the evaporation-induced self-assembly. Here, the ETPTA resin formed a thin layer near the contact line which can be seen clearly from the SEM images in Figure 4. It is noteworthy that these structures cannot be predicted from Surface Evolver by adjusting the contact angle and the liquid volume. These odd structures were due to the swelling of amidine PS particles by absorbed ETPTA monomers. Sheu et al. proposed a thermodynamic model for the swelling of cross-linked polymer particles by considering the chemical potential ( $\Delta\bar{G}_{m,p}$ ) of mixing, the elastic energy of the particles, and the water–particle interfacial energy:<sup>18,19</sup>

$$\Delta\bar{G}_{m,p} = RT[\ln(1 - v_p) + v_p + \chi_{mp}v_p^2] + RTN_cV_m(v_p^{1/3} - 1/2v_p) + 2V_m\gamma/a \quad (1)$$

in which  $R$  is the gas constant,  $T$  is the absolute temperature,  $v_p$  is the volume fraction of polymer in the swollen particle,  $\chi_{mp}$  is

(38) Battersby, B. J.; Lawrie, G. A.; Johnston, A. P. R.; Trau, M. *Chem. Commun.* **2002**, 1435–1441.

(39) Trau, M.; Battersby, B. J. *Adv. Mater.* **2001**, *13*, 975–979.

(40) Battersby, B. J.; Bryant, D.; Meutermans, W.; Matthews, D.; Smythe, M. I.; Trau, M. *J. Am. Chem. Soc.* **2000**, *122*, 2138–2139.

(41) Carter, W. C. [http://pruffille.mit.edu/~ccarter/tms\\_evolver\\_paper/tms\\_paper/tms\\_paper.html](http://pruffille.mit.edu/~ccarter/tms_evolver_paper/tms_paper/tms_paper.html).



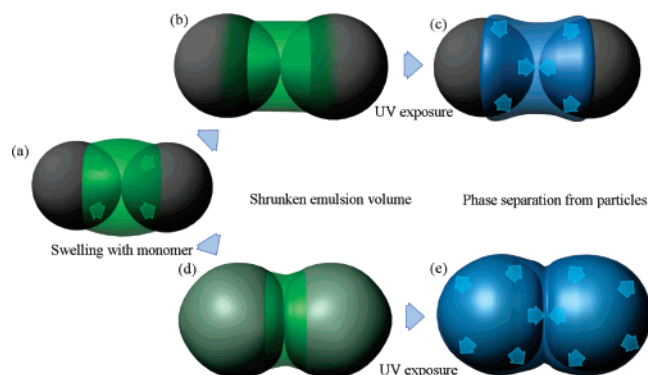


**Figure 5.** Schematic illustration of the formation of colloidal clusters with different morphologies depending on the degree of swelling.

the monomer–polymer interaction parameter,  $N_c$  is the effective number density of chains in the network,  $V_m$  is the monomer molar volume,  $\gamma$  is the interfacial energy between the particle and water, and  $a$  is the radius of the swollen particle. Although the amidine PS molecules in the colloidal particles were not cross-linked in this experiment, the theory can be applied conceptually to estimate the degree of swelling. Amine groups have a little bit higher affinity to the ETPTA monomers compared with sulfate groups according to the solubility parameters contributed from dispersion and polar forces.<sup>42</sup> Therefore, amidine PS particles are more likely to be swollen by ETPTA monomers than the PS particles with sulfate groups. More importantly, the number-averaged molecular weights of amidine PS and PS with sulfate groups were 9029 (PDI 3.765) and 90 152 (PDI 2.733), respectively. Consequently, amidine PS with a low molecular weight had a weaker elastic energy. When the swollen PS particles were exposed to a UV source, the difference in the free volumes of PS and cured ETPTA induced phase separation of the ETPTA from the PS particles.<sup>18,21,43,44</sup> However, it should be noted that the density of the amine groups was not enough to induce complete swelling because of the low concentration of the comonomer AEMH used in dispersion polymerization. Under these circumstances, the absorbed ETPTA monomers with insufficient affinity could not penetrate well into the PS particles but resided only in the vicinity of the contact regions of the PS particles. In this case, the absorbed ETPTA monomers were phase separated from the PS particles during UV exposure and formed thin layers around the contacting valley regions of the clusters. A schematic of the formation of thin ETPTA layers on the amidine PS clusters is illustrated as the route from (a) to (c) in Figure 5. Indeed, as shown in the SEM images in Figure 4, the resulting PS clusters were covered partially by a thin ETPTA layer, leaving a patch on the surface of each PS particle. Further, the PS clusters are similar to the minimal second-moment clusters, which were caused by the swelling-induced reduction of the emulsion volume.

Meanwhile, the PS particles with carboxyl groups are more likely to be swollen by the monomer than amidine PS particles due to higher affinity to the ETPTA monomers. The higher affinity is associated mainly with the solubility parameters of carboxyl groups and ester groups, considering that the molecular weight of PS with carboxylic groups is 8238 (PDI 3.612), which is similar to that of amidine PS.<sup>42</sup> With strong affinity, the ETPTA monomers could penetrate deeply into and swell the PS particles entirely. Also, the PS particles were packed closely through a critical packing under the action of compressive capillary forces

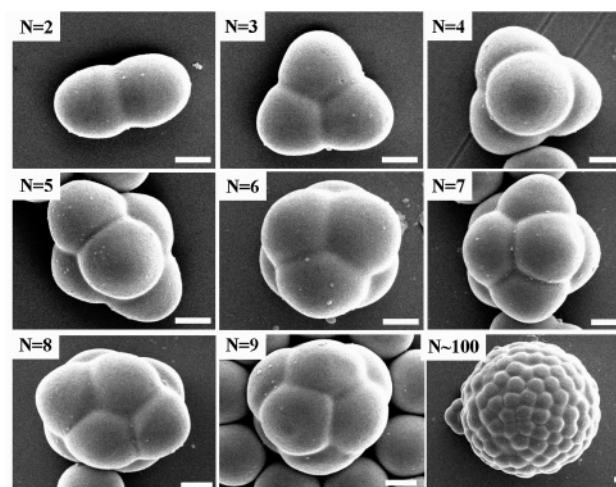


**Figure 6.** Collection of SEM images for composite clusters without patches of PS particles with carboxyl groups. The scale bar is 1  $\mu\text{m}$  in all images.

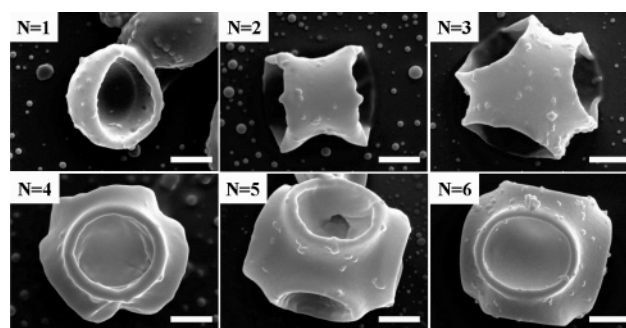


**Figure 7.** Collection of SEM images for ETPTA microparticles with coordinated large open windows formed by dissolving the PS particles from the patchy clusters of amidine PS. The scale bar is 1  $\mu\text{m}$  in all images.

as the ETPTA drop shrunk due to the monomer absorption. Because swollen PS particles are viscoelastic, they could be deformed under the capillary forces. During photopolymerization in the final stage, the absorbed ETPTA monomers which were present uniformly throughout the PS particles with carboxylic groups were phase separated in all directions as illustrated schematically in the route from (a) to (e) of Figure 5. Consequently, the ETPTA phase could not create patches on the clusters of the PS particles with carboxylic groups as shown in the SEM images of Figure 6.

Non-cross-linked PS particles can be dissolved by toluene, while UV-cured ETPTA is stable in toluene. When the patchy clusters of amidine PS particles were dispersed in toluene, the PS particles were removed from the clusters, leaving behind the ETPTA microparticles with large open windows. In Figure 7, the SEM images of these microparticles are shown for  $N = 1-6$ . Although the PS particles were contacting each other before photopolymerization, the contacting areas were blocked by phase separation of ETPTA during UV exposure without leaving interconnecting windows. The edges of the microparticles were blunt as compared with the sharp contact lines of the patchy clusters because of deformation induced in the absence of the supporting PS particles.

When the ETPTA emulsion contained rhodamine B of about  $10^{-4}$  M, dye-doped patchy clusters were obtained following the same procedures. Distribution of the dye molecules in the structure was analyzed with a laser scanning confocal microscope, and the resulting images are reproduced in Figure 8. As noted, a weak fluorescing intensity was observed from the PS particles because

(42) Van Krevelen, D. *Properties of Polymers*, 3rd ed.; Elsevier Science: Amsterdam, The Netherlands, 1997; Chapter 7.

(43) McMaster, L. P. *Macromolecules* **1973**, *6*, 760–773.

(44) Bates, F. S. *Science* **1991**, *251*, 898–905.

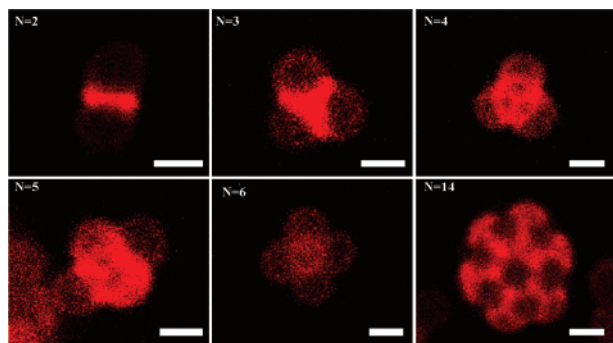


**Figure 8.** Collection of laser scanning confocal microscope images for rhodamine B-doped patched clusters. The scale bar is 2  $\mu\text{m}$  in all images.

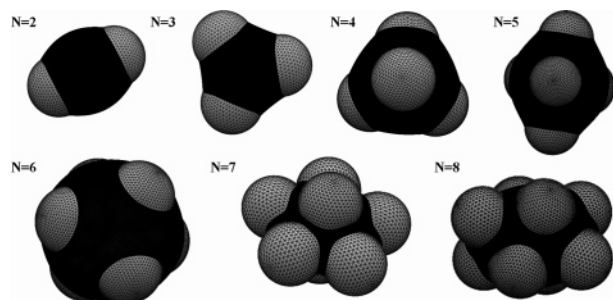


**Figure 9.** Images of the patched clusters with the packing configuration modeled by Surface Evolver. Here, each configuration corresponds to two-particle aggregates ( $N = 2$ ) at  $V/V_p = 1.44$ , triangles ( $N = 3$ ) at  $V/V_p = 1.04$ , tetrahedrons ( $N = 4$ ) at  $V/V_p = 1.64$ , triangular dipyrramids ( $N = 5$ ) at  $V/V_p = 2.33$ , octahedrons ( $N = 6$ ) at  $V/V_p = 3.05$ , pentagonal dipyrramids ( $N = 7$ ) at  $V/V_p = 0.58$ , and snub disphenoids at  $V/V_p = 1.32$  ( $N = 8$ ).

the dye molecules diffused into the PS particles slightly. However, most of the dye molecules were still in the cured ETPTA matrix, and the intensity from the interstices between the PS particles was much stronger than that from the PS particles.

**Surface Evolver Simulation for Patchy Particles.** Surface Evolver determines the minimum energy state that corresponds to the most favorable structure of the patchy cluster for a given emulsion volume and number of particles in the case of nonswelling particles.<sup>45</sup> Using Surface Evolver, Lauga and Brenner modeled the evaporation-induced dense packing of particles confined on the emulsion interface that was experimentally obtained by Manoharan et al.<sup>25,26</sup> Here, we performed the modeling of UV-induced patchy clusters for  $N = 1$ –8 by modifying the original Surface Evolver code developed by Lauga et al. Here, we assumed that all particles were anchored on the emulsion interface with the contact angle at  $150^\circ$  and exhibited repulsive hard-sphere interactions. Therefore, the particles did not interact until they contacted each other. Surface Evolver simulation found the particle configuration by minimizing the total energy, which was the sum of the interparticle potential and all surface energies contributed from particle–oil, particle–water, and oil–water interfaces. In Figure 9, some of the simulated patchy clusters were reproduced for  $N = 2$ –8 when the ETPTA drop volume was sufficiently small that the colloidal microspheres came into close contact. As noted, the particles were packed into the minimal second-moment configurations as the experimentally observed clusters in Figures 4 and 6.

From the simulation, the total surface energy scaled by the water–oil interfacial energy of unit area is plotted in Figure 10a as a function of the emulsion volume scaled by the volume of

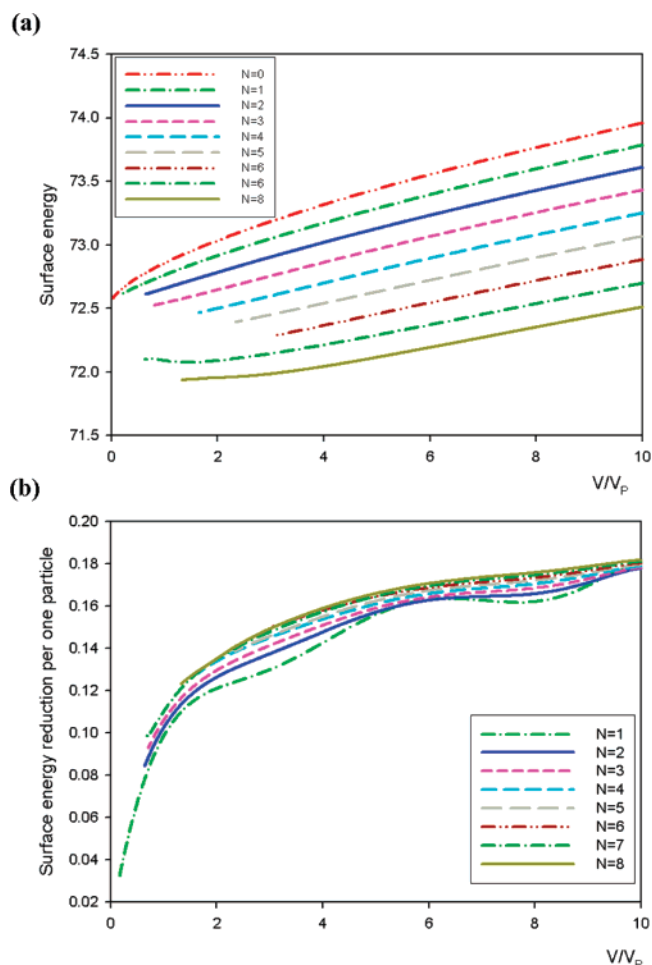


**Figure 10.** (a) Surface energy as a function of the emulsion drop volume for  $N = 0$ –8. (b) Normalized surface energy reduction per adsorbed particle as a function of the emulsion drop volume for  $N = 1$ –8. The normalized surface energy reduction on a flat interface is 0.264.

a single particle for  $N = 0$ –8. In this simulation, the system included eight particles and one emulsion drop for all cases to examine the surface energy reduction associated with both the particle adsorption and the decrease in the emulsion volume. For example,  $N = 5$  means that five particles were anchored on the interface and three particles were suspended freely in the water phase. Unlike our expectation, the curves did not intersect each other and were nearly parallel. This is due to the fact that the additional particle anchoring can reduce the total surface energy for a given drop volume. However, there were many clusters with a small number of particles in the experimental result because low accessibility to the jammed interface and considerable lubrication resistance prevented the particles from anchoring in the real situation.

Surface energy reduction by particle anchoring on a small emulsion droplet is different from the case of a flat interface. For a flat interface, the particles can reduce the surface energy by anchoring without deforming the flat interface.<sup>29,31</sup> Energy reduction can be simply calculated by the surface energy difference between two states, the anchored state and the unanchored state, and expressed as

$$E_b = \pi a^2 \gamma_{ow} (1 - \cos \theta)^2 \quad (2)$$

in which  $a$  is the particle radius,  $\gamma_{ow}$  the interfacial tension, and  $\theta$  the contact angle measured from the water phase. This equation

is also a good approximation for large spherical emulsions. However, the energy reduction depends on the emulsion volume when the emulsion size is on the order of the particle size. It is a simple matter to calculate the energy difference between anchored and unanchored states in a spherical interface and the normalized energy reduction by an adsorbed single particle, which is the total energy reduction divided by the number of adsorbed particles. In Figure 10b, the normalized energy reduction is plotted for  $N = 1-8$  as a function of the volume ratio. The normalized energy reduction was a weak function of the number of particles due to the differences in the interface shapes and became lower for a smaller emulsion drop. For a flat interface, the normalized energy reduction scaled by the water–oil interfacial tension can be simply calculated from eq 2, and the result is 0.264, which is much larger than the normalized energy reduction in Figure 10b for an emulsion drop interface. Therefore, particle adsorption is less favorable on smaller emulsion drops.

### Conclusions

We demonstrated a simple strategy for fabricating patchy colloidal clusters from a particle-stabilized Pickering emulsion. Specifically, we prepared an oil-in-water Pickering emulsion using UV-curable ETPTA oil as the emulsion phase and an aqueous PS suspension as the continuous phase. The structures of the particle-armored Pickering emulsions were captured by

UV irradiation in a few seconds to produce patchy particles. The size of the patches depended on the volume of the emulsion drop and the surface properties such as the contact angle. Low-molecular-weight PS particles with a high affinity to the ETPTA monomers tended to be swollen by the absorbing ETPTA monomers and produced composite PS clusters without patches. In this case, the structures were different from those for the minimal surface energy states. Also, dye-doped clusters were obtained by using ETPTA resin containing dye molecules. In some cases, the PS particles were removed by selective dissolution with toluene from composite PS clusters partially covered with ETPTA, which left behind ETPTA microparticles with coordinated large open windows. In addition, Surface Evolver simulation was performed to predict the structures of patchy clusters and the surface energy reduction by the particle adsorption as a function of the emulsion drop volume.

**Acknowledgment.** This work was supported by a grant from the Creative Research Initiative Program of the Ministry of Science & Technology for “Complementary Hybridization of Optical and Fluidic Devices for Integrated Optofluidic Systems”. We also appreciate partial support from the Brain Korea 21 Program and thank Dr. Eric Lauga at MIT for the Surface Evolver code.

LA703037G